Russian Apartment Building Thermal Response Models for Retrofit Selection and Verification

Peter Armstrong, Jim Dirks, Ray Reilly, Bill Currie, Ron Nesse (BNW[1])
Oleg Komarov and Boris Nekrasov (FER[2])

ABSTRACT

The Enterprise Housing Divestiture Project (EHDP) aims to identify cost-effective energy efficiency and conservation measures for Russian enterprise-owned apartment buildings and to implement these measures in the entire stock of buildings undergoing divestiture in six cities. Short-term measurements of infiltration and exterior wall heat-loss coefficient were made in the cities of Cheropovets, Orenburg, Petrozavodsk, Ryazan, and Vladimir. Long-term monitoring equipment was installed in six or more buildings in each of the aforementioned and in the city of Volxhov. The results of these measurements will be used to validate models for selecting optimal retrofit packages and to verify energy savings. The retrofit categories representing the largest technical potential in these buildings are envelope, heat recovery, and heating/hot water system improvements. This paper describes efforts to establish useful thermal models to aid in retrofit selection and for measuring the savings generated by completed retrofits. The model structures and analytical methods for obtaining building parameters from time series weather, energy use, and thermal response data are developed. Our experience applying these methods to two nominally identical 5-story apartment buildings in the city of Ryazan is presented. Building envelope UAs inferred from measured whole-building thermal response data are compared with UAs based on U-values obtained by ASTM in-situ measurements of 20 Ryazan wall sections. The UAs obtained by these independent measurements differ by less than 7%.

INTRODUCTION

In the Soviet economy, housing and social services were provided for workers' families by industry as a part of the cost of production. Enterprises built, operated, and effectively owned housing. The post-soviet Russian government is striving to build a market economy. Enterprises must divest social assets, and markets for social services, particularly housing and associated support services such as building maintenance, are encouraged. However, existing buildings are viewed as a risky investment, in part because of their high energy use intensities and the poor condition of their envelope, heating, water service, and waste water systems (Martinot 1997). The Enterprise Housing Divestiture Project (EHDP) is providing loans and technical guidance for revenue metering and for envelope and technical systems improvements to apartments undergoing divestiture in each of six participating cities. The Technical Advisory Group (TAG) has been tasked with developing and demonstrating the engineering measurement and analysis elements of the program. The TAG has worked closely with Russian counterparts who will ultimately extend the program to the several hundred thousand Russian dwelling units that are expected to obtain EHDP retrofits at a cost of about 500M$ (Whittle et al. 1996).

---

[1] Battelle, Pacific Northwest Division, Richland, Washington.
[2] Foundation for Enterprise Restructuring and Financial Institutions Development, Moscow, Russia.

With so large an investment, it is important to carefully identify and ensure correct installation and operation of the most cost-effective technologies applicable to Russian building types and conditions. First, it is necessary to understand Soviet architecture, the distribution of building types, the operating environment, and how their technical systems *actually perform in the field*. Second, effective audit and metered data collection protocols are needed to estimate potential and realized savings. Third, selection of life-cycle cost-optimal packages of heating retrofits requires thermal analyses (bin-method or transient simulation) appropriate to the EHDP building systems/operations to properly account for changes in balance point, thermal mass effects, and the interactions of retrofit measures (Dirks et al. 1996). Finally, to ensure correct installation and operation of measures through several years of ESCO procurement cycles, it is important to establish and apply effective, multi-tiered acceptance test methods, verification protocols, and ongoing program evaluation.

A survey of enterprise- and municipal-owned housing was prepared during EHDP pre-appraisal missions in 1995. Candidate EHDP cities included Novocherkassk, Orenburg, Petrozavodsk, Ryazan, Vladimir, and Volxhov at the time of the survey. Size, basic construction, and energy source data for the housing stock in these cities are summarized in Table 1. Cheropovets later replaced Novocherkassk, and the target building set was reduced to about one-half of the 5-story and higher buildings only.

Table 1. Stock of Enterprise and Municipally Owned Housing in Six Cities

Construction Type	Height (stories)	space/service water heat source[b]			Total Buildings	Total Apartments[c]	Total Floor Area[c] (m²)
		both gas	SWH by gas	both DH			
1-2 family[a]		343	783	193	1,319	1,980	89,100
Wood	2 to 4	0	1,945	2,193	4,138	82,760	4,138,000
Brick	2 to 4	75	831	2,958	3,864	77,280	3,864,000
Brick	5	0	549	986	1,535	92,100	4,605,000
Panel	5	0	276	2,450	2,726	163,560	8,178,000
Brick	6 to 8	0	0	247	247	22,230	1,111,500
Panel	6 to 8	0	0	0	0	0	0
Brick	9	0	0	688	688	96,320	4,816,000
Panel	9	0	0	1,698	1,698	237,720	11,886,000
Brick	10 to 13	0	0	260	260	29,900	1,495,000
Panel	10 to 13	0	0	94	94	10,810	540,500
Brick	14 & over	0	0	28	28	4,480	224,000
Panel	14 & over	0	0	42	42	6,720	336,000
Subtotal	5 & over	0	825	6,493	7,318	663,840	33,192,000
Total	All	418	4,384	11,837	16,639	825,860	41,283,100

[a]brick and wood construction are both included in the '*1-2 family*' category.

[b]heat sources are district heat (DH) and gas; SWH (service water heating) is sometimes provided by apartment-level gas water heaters even in buildings with district heated radiators; buildings listed in the '*both gas*' column are generally found in low-density housing areas beyond the reach of DH networks.

[c]estimates based on typical apartment floor areas, typical section plans, and reported building counts.

Well over half the EHDP floor area resides in two building types: 5- and 9-story panel buildings. The six panel buildings selected for testing in 1995 therefore include three identical 5-story, four-section buildings at Zubkova 22-1, 24-3, and 24-3, each housing 60 apartments with

gross floor area of 4056 m^2 and three 9-story, four-section buildings at Novoselov 30, 32, and 34, each housing 144 apartments with gross floor area of 10417 m^2. The buildings were constructed in the early 1980s of concrete panels cast locally in Ryazan.

Panel buildings typically have 35-cm-thick exterior panels and 1.5-m-high by 2-m-wide standard window units each containing three double-glazed operable sash panels of nominal 1.5 x 1.5, 1.0 x 0.5 and 0.5 x 0.5 m size. Small bedrooms and kitchens sometimes use a smaller (1.5 x 1.5 m) standard window. The apartment building at Zubkova 22-1 is shown in Figure 1. Panels are attached by welding metal tabs that protrude at standard locations along their edges. A typical exterior panel wall is shown before grouting in Figure 2. After welding, the panel joints are filled with grout, which is sometimes covered with mastic or a similar sealant.
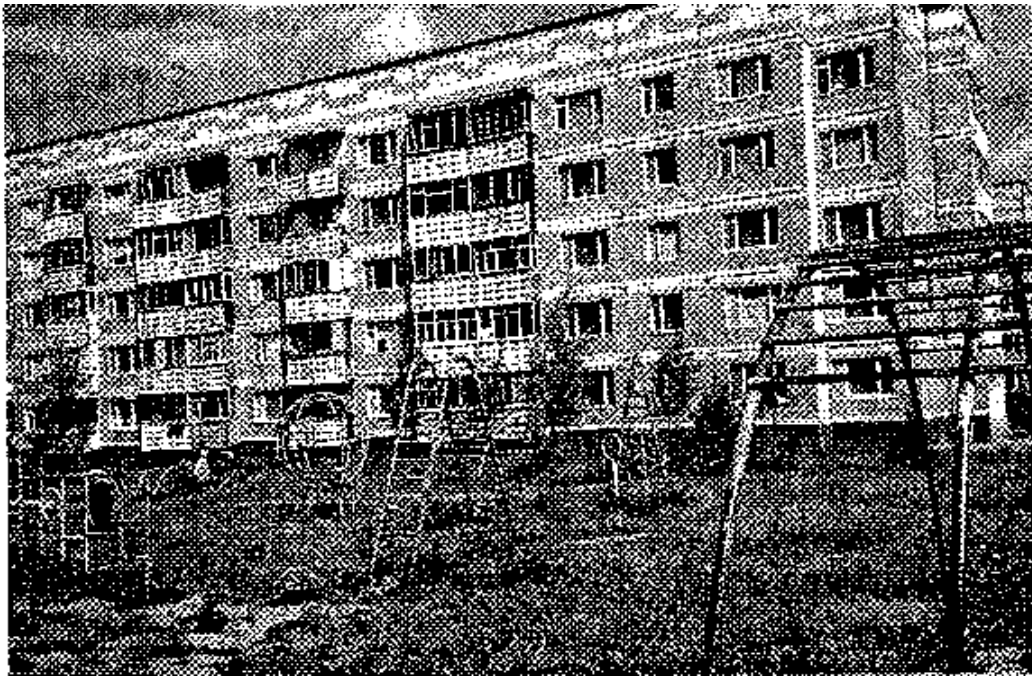

Figure 1. 5-Story Apartments of Panel Construction, Zubkova 22-1, Ryazan

Each apartment typically has a balcony accessed from the main room by a partly or fully double-glazed door. The main room has an additional window in rare cases. All other rooms, including the kitchen have a single standard window unit. The bathroom is an exception (bathrooms are never situated on an exterior wall). There is a hot water radiator under each window. All six of the monitored buildings have attics. Except for the double-glazing of windows and the reported use of light aggregates in exterior panels, most EHDP building envelopes are uninsulated. A *one-room apartment* has a kitchen, bathroom, and one main room and a floor area of 30 to 35 m^2; a *two-room apartment* has one additional room and a floor area of 48 to 54 m^2; and a *three-room apartment* adds yet another room for a floor area of 67 to 73 m^2.

Heat, service, and wastewater risers are exposed in apartments as they traverse the vertical extent of a building. Electrical risers, on the other hand, pass through a chase and the treatment of floor penetrations varies. Doors and windows, passive ventilation channels, smoke control channels, electrical chases, and stair and elevator shafts are the main paths available for air movement into, out of, and through the building.
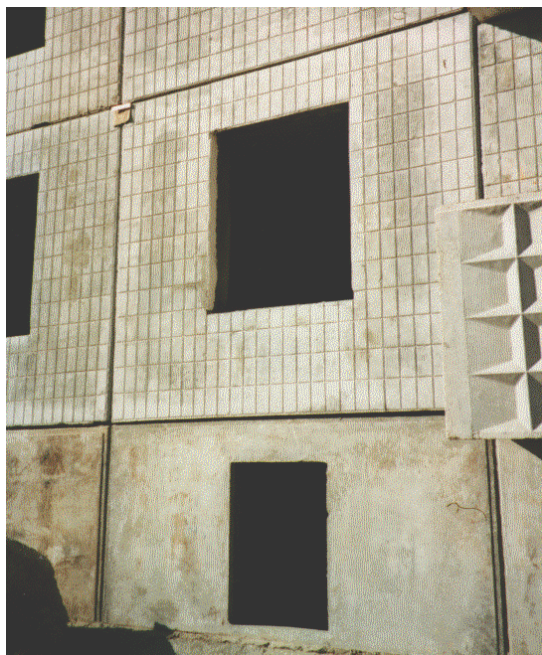
Figure 2. Typical Panel Building Under Construction

ENVELOPE COMPONENT TESTING AND ANALYSIS

The cost effectiveness of an energy efficiency measure is first-order sensitive to fuel cost, cost and performance of the measure, and the existing condition of the energy subsystem to which the retrofit is applied. Fuel prices, conversion efficiencies, and retrofit installation costs are known or can be estimated with reasonable confidence. The performance of an existing energy using subsystem, on the other hand, is often not well known and can vary considerably by region and even among nominally identical buildings. Audits of all participating buildings, tests of a large subsample, and long-term monitoring of a smaller subsample are needed to reliably establish existing building conditions.

Blower Door Tests. Whole apartment blower door testing was performed in 48 occupied apartments in 1995 (Armstrong et al. 1996). The equivalent leakage areas (ELA) attributed to windows in over half of these apartments were between 12 and 33 cm^2 per window unit (modern western window ELA is typically less than 1 cm^2). Additional testing was performed in Ryazan (1996-97) and Vladimir (1997) to determine the ELA contributions of specific building elements such as floor joints in first- and higher-floor apartments, ceiling joints in top- and lower-floor apartments, interior and exterior wall panels, exterior brick walls, and apartment doors. Additional testing in Ryazan determined the effectiveness of various types of window weather stripping, the leakiness of ventilation shafts, and the magnitudes of hidden leaks associated with clearance gaps that surround prefabricated bathrooms (BNW 1997b). Results are summarized in Table 2.

Table 2. Typical Equivalent Leakage Areas (cm^2) by Envelope Component

(sub)Component	Unit ELA (cm^2)	Total ELA (cm^2)
Window Assembly (4), summer	**111.5**	**446**
winter	**58**	**210**
glass-to-sash perimeter	*5.5*	*22*
sash-to-frame perimeter (summer)	*80.5*	*322*
sash-to-frame perimeter (winter)	*21.5*	*86*
frame-to-wall perimeter	*22*	*88*
window sill	*3.5*	*14*
Prefabricated Bathroom (1)	**230**	**230**
accessible for sealing	*195*	*195*
water/sewer pipes	*76*	*76*
Concrete Apartment Envelope	**NA**	**204**
exterior wall panel joint (4)	*7*	*28*
exterior wall panel pore (4)	*4.3*	*17*
interior wall panel joint (2)	*2*	*4*
interior wall panel pore (2)	*3.2*	*6*
floor perimeter (5)	*24*	*120*
floor joints and pores (5)	*3.8*	*19*
ceiling joints (5)	*1.9*	*10*
Utility Penetrations	**NA**	**94**
ceiling light fixture (6)	*6.3*	*38*
radiator riser pipes (5)	*4*	*20*
wall switch (6)	*6*	*36*
Entry Door to Apartment	**36**	**36**
Apartment ELA, no window weather stripping		**1026**
ELA with typical winter weather stripping		**790**

Infiltration and Ventilation Heating Loads. The heating load represented by infiltration is a function of envelope leakiness, wind pressure, and temperature difference. ASHRAE (1993) recommends for low-rise detached houses a two-term quadrature model in which the coefficients of temperature difference and wind pressure terms are functions of size and spatial distribution of envelope leaks. Detailed modeling of air flow in 5-, 9-, and 16-story prototypical EHDP buildings (BNW 1998a) led us to adopt an extended quadrature model.

Weatherization measures can be applied to a variety of leaks at various locations. To characterize weatherization impacts, a seven-dimensional Latin hypercube design was used to represent leakiness space. The two extremes of each condition (very leaky and very tight) were represented in the test grid. This gives $2^7=128$ leakiness conditions for each building. In addition, the intermediate conditions for six (all except vent riser leakiness) leakiness dimensions were considered in certain combinations. The result is an experimental design in which the vertices and intermediate points on the edges are represented, but the mid-points of the hypercube faces are not. The three (two extreme plus intermediate) values of each envelope component are documented in Appendix E of (BNW 1998a).

For each leakiness condition, the infiltration rates were calculated at each of 25 wind pressure (0, 3, 6, 12, and 24 m/s) and temperature difference (0, 12.5, 25, 37.5 and 50 K)

points. The exponent and coefficient (x_t, C_t) in the temperature difference term were evaluated by the blower door data analysis method (linear least squares fit of log-transformed power law) using the five points with zero wind pressure. The wind pressure exponent and coefficient (x_w, C_w) were similarly evaluated using the five points where temperature difference is zero. The grid points were weighted according to the approximate contribution to annual infiltration heating load represented by the temperature-wind speed bin associated with each grid point. A quadrature equation involving the wind-temperature product, as well as wind and temperature terms, was fit to over 10,000 airflow model solutions (BNW 1998a).

U-Value Test Protocol. The cost-effectiveness of adding exterior insulation is first-order sensitive to the U-value of the existing wall. Russian standards have, for many years, called for exterior panel fabrication employing various insulation means such as a three-layer pour with a middle layer of aerated and/or low-conductivity aggregate concrete (Drozhdov et al. 1989; Matrosov et al 1994; Opitz et al. 1997). A number of reliable Russian sources reported that these provisions of the standards were frequently ignored. The TAG was therefore tasked to perform in-situ U-value tests on typical walls, attic floor decks, and 1st-floor decks.

Tests were conducted in a total of 74 apartments distributed among 23 buildings in Zhukovskij, Ryazan, Petrozavodsk, and Orenburg (BNW 1998b). Most tests were performed in winter and early spring with outside temperatures of +5°C or less. Two to four heat flux meters (HFMs) were installed per apartment and monitored for 3- to 4-day test periods.

The exterior wall of each room usually has one large centrally located window surrounded by 50 to 120 cm of masonry wall on all sides, as shown in Figure 2. In some cases one or two of up to four test points per apartment were set up on an adjacent windowless wall (gable wall or small panel section facing a balcony). Locations for installing heat flux meters were restricted to positions roughly equidistant from the panel's outer edge and the window frame to minimize lateral heat flow—i.e., locations where heat flow is nearly perpen-dicular to the wall surface. Radiators and pipes also had to be avoided because lateral heat flows are strong near any local heat source. Thermographic images (Zhuze 1996) of exterior surfaces clearly showed the warm areas corresponding to radiators and riser pipes, but showed no evidence of thermal bridging or of areal non-uniformity in panel conductance. North- or northeast-facing walls were favored in the selection of U-value test locations to obtain the largest possible temperature difference and wall-normal heat flux.

Similar installation schemes were used for floor and roof tests. The installer looked for cold (generally windward) sections of the basement before entering a building to recruit a test apartment for floor tests. The basement ceiling acted as the outside surface for such tests. The heat flux sensor was installed under a carpet in one case and on the bare floor surface in all others. Attic U-value tests presented the difficulty of running a leadwire to the roof and attaching the thermocouple in icy and windy conditions, in addition to the usual difficulties of recruiting top-floor tenants. The tests were therefore limited to measuring the U-values of the top-floor ceiling-panel. Insulation was not present on the attic floor in any of the tested buildings.

U-Values Test Results. Surface temperature and heat flux histories from a typical 3-day test in Petrozavodsk are shown in Figure 3. Short test duration, and the strong transients typically experienced, necessitated development of an improved U-value analysis method for the project (Appendix A). The test results are shown as distributions of U-values, by wall category, in Figure 4. Note that the median measured U-values of brick walls exceed all

those measured for panel walls. Gable panel walls have the lowest U-values. The thin floor and ceiling sections have the highest measured U-values.   Table 3 shows the median measured U-values (W/m^2·K) and sample standard deviations for all 12 categories of envelope component tested. Figure 4 indicates significant variation across cities for the U-values of most of the envelope components. It was hypothesized that some of the variation in U-values might be caused by the height or the age of the building. However, no such correlation was found with height or year of construction.
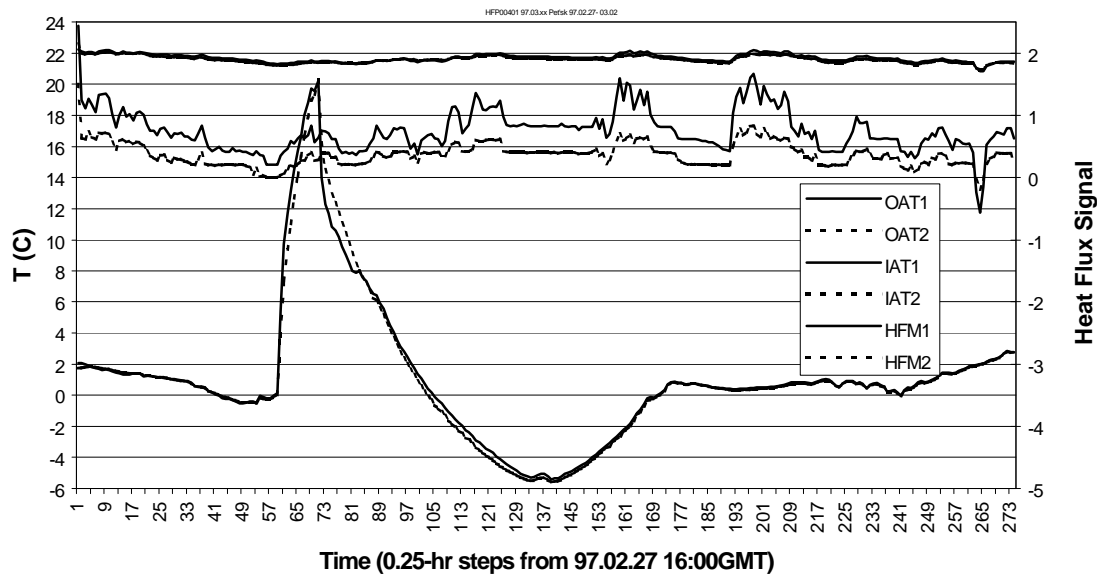
Figure 3. Contemporaneous U-Value Test Data from Two Locations on One Wall, Both Showing Strong Transient Excitations and Responses

The U-value estimates were compared with U-values given for concrete walls used in North American construction (ASHRAE 1993). For example, the median of the measured U-values in Zhukovskij corresponds to a wall density close to 1,600 kg/m^3, which corresponds to concrete with moderately light aggregate. The panels in other cities are apparently denser than the Zhukovskij panels or differ significantly in other aspects that affect U-value. The very systematic factor-of-two difference in the measured values for Petrozavodsk window panels and gable panels suggests that different designs and/or materials were used consistently to obtain lower U-values for the gable ends in this northernmost of EHDP cities. The observed U-value variation among cities implies that there are systematic inter-city design or materials differences as well. Measured U-values (1÷resistance) are combined (sum of resistances) with their appropriate inside and outside air films for use in heat loss calculations. Table 3 shows the resulting overall U-values.

The addition of surface film resistances decreases the dispersion in the values because a wall *per se* has such low thermal resistance that overall thermal resistance is dominated by the film resistances. The cumulative relative frequency distribution for each of the different wall categories (attic floors and basement ceilings including film resistances) are shown in Figure 5. Because the horizontal surfaces (floors and ceilings) are not directly exposed to ambient (i.e., they are exposed to the basement and attic), there is no wind and the "outside" film resistance is much greater.
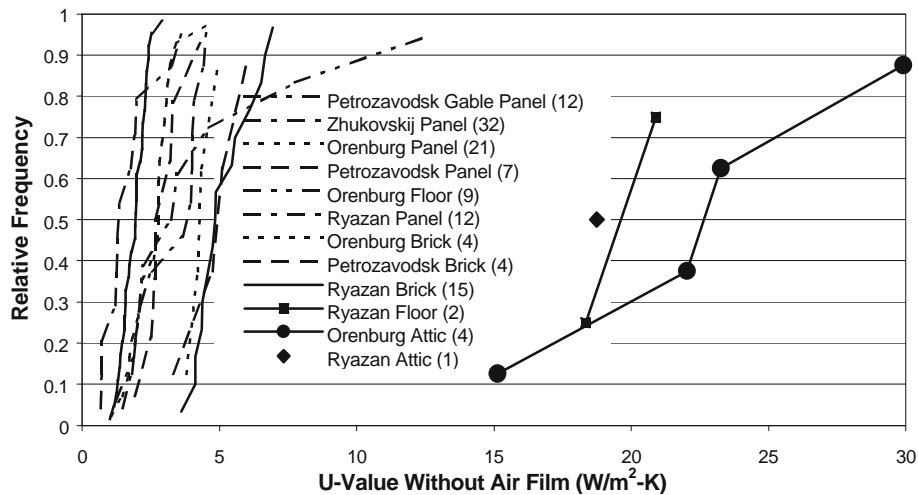
Figure 4. U-Value Cumulative Distributions by City and Wall Type

Table 3. U-Values Including Air Films

	Median U-Value Without Air Film $(Wm^{-2}K^{-1})$	Sample Standard Deviation $(Wm^{-2}K^{-1})$	Component Thermal Resistance (m^2KW^{-1})	Air Film Resistance Inside (m^2KW^{-1})	Air Film Resistance Outside (m^2KW^{-1})	Total Resistance (m^2KW^{-1})	Median U-Value With Air Film $(Wm^{-2}K^{-1})$
Orenburg Panel	2.76	0.79	0.362	0.1206	0.0293	0.512	1.95
Petrozavodsk Gable Panel	1.31	0.96	0.763	0.1206	0.0293	0.913	1.10
Petrozavodsk Panel	2.66	0.76	0.376	0.1206	0.0293	0.526	1.90
Ryazan Panel	3.81	1.14	0.262	0.1206	0.0293	0.412	2.42
Zhukovskij	1.95	0.46	0.513	0.1206	0.0293	0.663	1.51
Orenburg Brick	4.27	0.46	0.234	0.1206	0.0293	0.384	2.60
Petrozavodsk Brick	4.74	1.12	0.211	0.1206	0.0293	0.361	2.77
Ryazan Brick	4.85	1.03	0.206	0.1206	0.0293	0.356	2.81
Orenburg Floor	3.24	3.64	0.309	0.1631	0.1631	0.635	1.57
Ryazan Floor	19.62	1.82	0.051	0.1631	0.1631	0.377	2.65
Orenburg Attic	22.64	6.06	0.044	0.1080	0.1080	0.260	3.84
Petrozavodsk Attic	18.75	NA	0.053	0.1080	0.1080	0.269	3.71

Median measured U-values for all wall types are compared with handbook (ASHRAE 1993 Table 22.4) values for similar materials in Table 4. The values generally compare quite well. For example, the Petrozavodsk gable end panels and the Zhukovskij panels have low U-values corresponding to concretes made with low-density ("expanded shale, clay, or slate; expanded slags") aggregates. It is also possible that these panels have a two- or three-layer construction in which one of the layers is made with a very low density aggregate (LDA) and the others are common ("gravel or stone aggregate") concrete. The Petrozavodsk front- and back-wall panels and all panels tested in Ryazan and Orenburg had U-values corresponding to common concrete. Note that panel tests represent over 2/3 (84 of the 123) U-value measurements. Measured brick walls median U-values, on the other hand, are about twice the handbook value quoted for heavy clay brick[3]. The thickness of brick walls makes the U-

---

[3] The *Handbook* indicates that the thermal properties of mortar and heavy clay brick are very close.
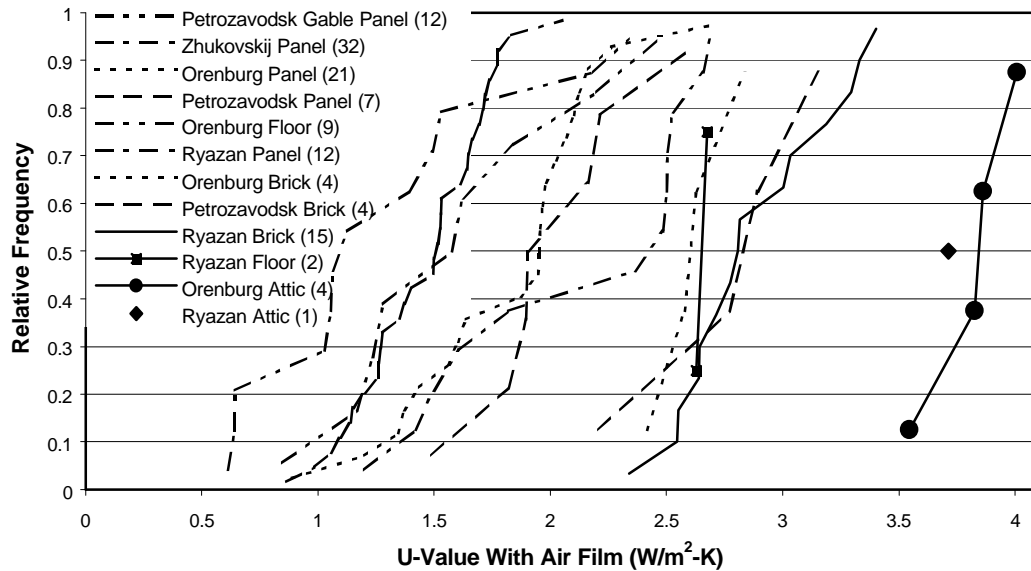
Figure 5. U-Values With Film Resisance—Distributions by City and Wall Type

value measurements much more susceptible to lateral heat transfer. We believe that the measured brick wall U-values are biased from drapes shielding part of the wall near, but not over, the heat flux sensor, and by the fact that exterior wall area is well over 1.5 times the projected area because of the exposed surface area associated with the window recess.

There are no reports in the U-value measurement literature of field measurements on thick, massive apartment building walls, and the U-value test results are not consistent with published Russian standards. Reconciliation of representative measured U-values with the corresponding whole-building thermal performance measurements was therefore pursued.

Table 4. Measured and Handbook U-Values (without air film resistances)

	Median $(Wm^{-2}K^{-1})$	$k_{eff} = t \cdot U$ $(Wm^{-1}K^{-1})$	Standard Error	N	Handbook Material	Density $(kg\ m^{-3})$	k $(Wm^{-1}K^{-1})$
Orenburg Panel	2.76	0.97	0.79	21	Concrete	1920	0.9-1.3
Petrozavodsk Gable	1.31	0.46	0.96	12	LDA concrete	1200	0.42-0.53
Petrozavodsk Panel	2.66	0.93	0.76	7	Concrete	1920	0.9-1.3
Ryazan Panel	3.81	1.33	1.14	12	Concrete	2080	1.0-1.9
Zhukovskij Panel	1.95	0.68	0.46	32	LDA concrete	1440	0.58-0.74
Orenburg Brick	4.27	2.78	0.48	4	Brick & mortar	2080-2160	1.2-1.5
Petrozavodsk Brick	4.74	3.08	1.12	4	Brick & mortar	2080-2160	1.2-1.5
Ryazan Brick	4.85	3.15	1.03	15	Brick & mortar	2080-2160	1.2-1.5
Orenburg Floor	3.24	See text	3.64	9	20-cm air gap	See text	
Ryazan Floor	19.62	2.94	1.82	2	Concrete	2400	1.4-2.9
Orenburg Attic	22.64	3.40	6.06	4	Concrete	2400	1.4-2.9
Petrozavodsk Attic	18.75	2.81	NA	1	Concrete	2400	1.4-2.9

WHOLE BUILDING THERMAL RESPONSE

Complete time series data were obtained for a large sample of apartment temperatures and for all utilities serving the 5-story demonstration buildings at Zubkova 22-1 and Zubkova 24-3 in Ryazan during most of the 1996-97 heating season. These were the only two demonstration buildings with gas meters operating consistently during the winter of 1996-97; both are served by the same district heating substation. From the data, we have derived models of transient heating load in response to indoor and outdoor temperature, solar radiation, wind, internal gains, and utility heat inputs.

Operational Differences. Figures 6 and 7 show the daily net heat inputs to 22-1 and 24-3 from all utilities (third trace) and the shares provided by cooking gas (area below the first, lowest trace), radiators (area between second and third traces), and other (area between first and second traces). The *other* category includes electrical power, service hot water recirculation through bathroom radiators, and enthalpy streams associated with hot and cold tap water use. Each tap water share is computed by taking the product of instantaneous flow rate and the corresponding supply-waste water temperature difference. The radiator heat term, as well as the hot and cold tap water terms, include distribution losses because they are monitored at the service entrance in each building's basement. The fourth trace shows indoor temperature[4], a daily average across 18 apartments in 22-1 and 19 apartments in 24-3.
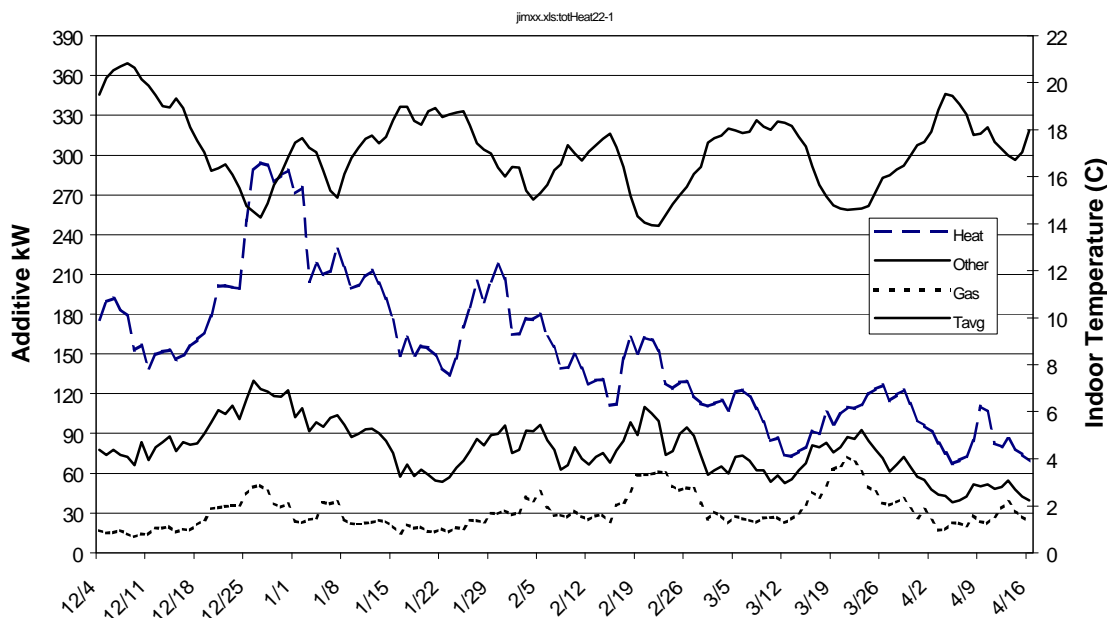

Figure 6. Average Daily Indoor Temperature and Total Daily Heating Inputs for all Sources Measured in Zubkova 22-1 from 4 December 1996. "Other" Includes Electrical Power, Service Hot Water Re-Circulation, and Hot and Cold Tap Water Net with Respect to Waste Water

---

[4] Temperature loggers were deployed in two 1st, 3rd, and 5th-floor apartments in each section of each building.
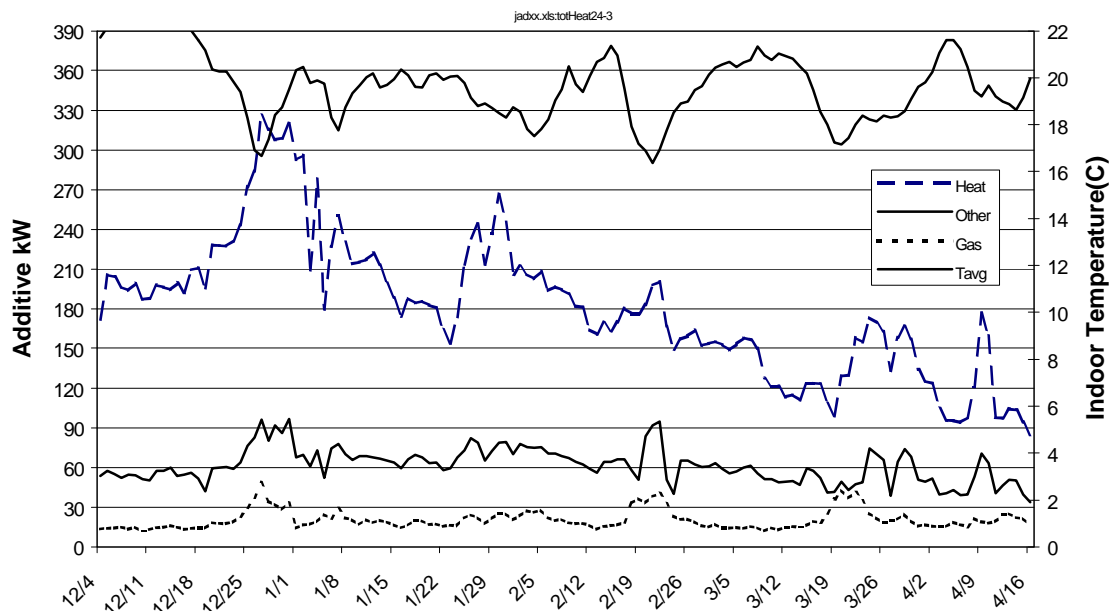
Figure 7. Average Daily Indoor Temperature and Total Daily Heating Inputs for all Sources Measured in Aubkova 24-3 from 4 December 1996

In the Ryazan demo buildings, the cold water enthalpy stream is typically larger in magnitude than the heat input by electric power. The reason is that cold water, entering at 3 to 5°C, is mainly used in the toilets and thus has a long residence time. Waste water typically leaves at temperatures close to room temperature. The seasonal average values of all the heat inputs are tabulated in Table 5. Note that average indoor temperature is significantly lower in 22-1 than in 24-3. Different heat control retrofits made in mid-1996 explain most of this difference. The average, maximum and minimum values of the daily mean outdoor temperature time series for 4 December 1996 to 16 April 1997 were -4.9, 10.9, and -27.5°C. Horizontal solar radiation averaged 63.2 W/m^2, and wind speed averaged 3.8 m/s (BNW 1997a).

Table 5. Average Temperatures and Heat Inputs 4 December 1996 – 16 April 1997

	units	Zubkova 22-1	Zubkova 24-3
Indoor Temperature	°C	17.1	19.7
Gas Stoves	kW	31.34	20.75
Electrical	kW	9.93	9.09
Heating System	kW	71.88	118.64
Hot Tapwater	kW	33.78	39.01
Cold Tapwater	kW	-10.07	-24.30
DHW Recirculation	kW	11.97	18.31
Net Thermal Power	kW	148.83	181.50

The radiators and distribution piping in 22-1 were flushed and balanced, piping was replaced as needed, and a heat exchanger and load-side pump were installed in place of the existing hydroelevator system. In 24-3, each of the four hydroelevators was replaced by a recirculation pump and a modulating valve, which controls the radiator loop supply

temperature in proportion to outdoor temperature. The maximum heat rate to 22-1 was therefore limited by the maximum heat exchanger primary-side flow at the pressure difference developed by the district heating network. The flow rate was lower after installation of the heat exchanger than it had been with the original hydroelevators.

In 24-3 the flow of entering district heating water could easily exceed the flow into the previous hydroelevator system when the valves were fully open. When district heat supply temperatures were below the values established by the district heating outdoor temperature reset schedule, the control system would compensate by letting in more water so that the tenants of 24-3 could stay warm while their neighbors shivered.

In 22-1 the cold tenants coped as best they could by drawing less cold tap water (partly achieved by toilet repairs made in mid-1996) and more hot water. The occupants of 22-1 also used their kitchen stoves to stay warm. Gas use is more than double that of 24-3 during periods of heat deficit—that is, at times when indoor temperatures are much below 18°C. The Zubkova buildings show dramatically that two nominally identical buildings can be operated such that their thermal behaviors bear very little resemblance.

Thermal Response Model. We based our model on a number of similar low order heat balance models (see Armstrong et al. 1991 literature review) from the literature. The full model has several additional terms to account for thermal storage, but its steady-state form conveys the essence:

$$Q + k_S*S = k_W*W*dT + k_T*dT$$

where

Q is net energy provided by gas, electric, people, and heat and water utilities (W),
k_S, k_W, k_T are evaluated from terms (Appendix B) of the transient model:
  k_S represents an effective (with respect to horizontal insolation) aperture area (m^2),
  k_W represents an infiltration admittance (W/K per m/s),
  k_T represents an overall envelope conductance or UA (W/K),
S is average solar radiation (Wm^{-2}) incident on the horizontal,
W is average wind speed (m/s),
dT is average indoor-outdoor temperature difference (K).

The model coefficients and fit statistics are listed in Table 6. The model of Zubkova 22-1 represents a UA of 7739 WK^{-1}, an effective solar aperture (including sol-air effects on opaque wall and roof surfaces) of 178 m^2 and a 22.3 kW average internal gain corresponding to about 159 full-time equivalent (FTE) occupants. The model of Zubkova 24-3 represents a UA of 7056 WK^{-1}, an effective solar aperture of 202 m^2 and 28.4 kW average internal gain corresponding to about 203 FTE occupants[5]. The time series of model residuals (modeled – measured total heat input) are plotted in Figure 8. Cumulative distributions of the residuals are seen in Figure 9 to be nearly Gaussian.

Reconciliation Of UA Estimates. The envelope areas, by component, were obtained from building plans and confirmed by field audit (Birch and Krogboe 1995). There are 50 small (kitchen) windows of 1.8 m^2 each, 100 large windows of 2.8 m^2 each, 40 balcony window/door units of 3.72 m^2 each, and 32 common space windows of 1.85 m^2 each.

---

[5] An occupant is assumed to dissipate 140 W.

Table 6. Terms and Standard Errors of the Whole-Building Thermal Models

Term	Units of coefficient	Zubkova 22-1 $r^2 = 0.975$			Zubkova 24-3 $r^2 = 0.932$		
		coefficient	std.error	t-ratio	coefficient	std.error	t-ratio
const	kW	22.33	16.61	1.34	28.36	38.04	0.75
Q_1	kW/kW	0.4443	0.0577	7.71	0.1679	0.0602	2.79
solar	m^2	177.89	39.40	4.51	202.51	61.33	3.30
W*dT	kW/Kms^{-1}	0.0951	0.0404	2.35	0.1253	0.0248	5.05
$T_{z,0}-T_{x,0}$	kW/K	19.93	3.06	6.52	33.31	3.79	8.79
$T_{z,1}-T_{x,0}$	kW/K	-15.52	2.73	-5.69	-27.11	3.51	-7.73
$T_{x,1}-T_{x,0}$	kW/K	-1.233	0.371	-3.33	-2.125	0.470	-4.52
UA	kW/K	7.94			7.45		

RUS\REPORTS\RZ\SEP97\RZUBCRTF2 980711pra
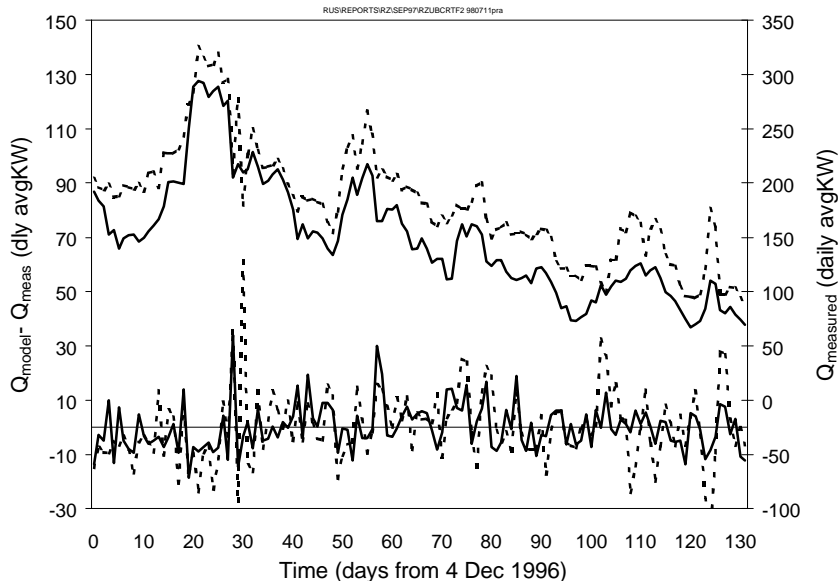
Figure 8. Net Heat Input Time Series for Zubkova 22-1 (Solid) and Zubkova 24-3 (Dash) with the Corresponding Model Residuals Shown Below
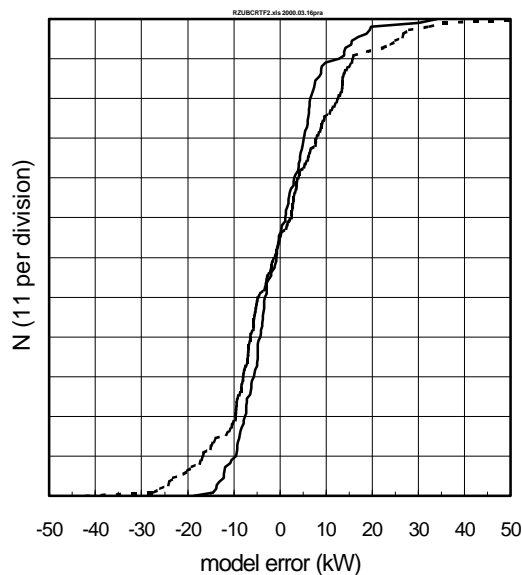

RZUBCRTF2.xls 2000.03.16pra

Figure 9. Cumulative Distribution of Residuals for 22-1 (Solid) and 24-3 (Dash)

The double glazed window with 1.5 cm air gap has an assumed U-value of 3.06 $Wm^{-2}K^{-1}$. Two-thirds of the balconies are assumed to be covered (tenant-installed glazing) with a lower U-value of 2.16 $Wm^{-2}K^{-1}$. Common-space windows are assigned a higher U-value of 3.69 $Wm^{-2}K^{-1}$. The resulting window area is 578 m^2 and the total UA for windows is 1716.7WK^{-1}.

The Table-4 U-values that can be applied to the demonstration buildings are 2.4245 $Wm^{-2}K^{-1}$ for the Ryazan wall panel, 2.6508 $Wm^{-2}K^{-1}$ for the Ryazan floor, and 3.8440 $Wm^{-2}K^{-1}$ for the Orenburg attic deck. The building perimeter, including indents, is 176.5 m and the height of the conditioned volume is 2.55*5 giving a net wall area of 2250 – 578 = 1672 m^2. The median wall U-value measured in Ryazan was 2.424 $Wm^{-2}K^{-1}$, giving a wall UA of 4053 WK^{-1}. The attic floor and basement ceiling each have an area of 811 m^2. These are buffer spaces heated, respectively, by ventilation system exhaust and hot water pipe losses. Based on typical temperatures measured in these spaces (BNW 1996, 1997a) we assign temperature differences from the interior to the attic and basement that are 1/10 and ½, respectively, of that experienced by the windows and walls. The assigned buffer characteristics lead to an effective attic UA of 301 WK^{-1} and an effective basement UA of 1075 WK^{-1}. The total envelope conductance is 7146 WK^{-1}.

The UAs obtained from the measured thermal responses of buildings 22-1 and 24-3 differ by less than 7%, and the UA obtained from the building dimensions and directly measured U-values adjusted by application of handbook film coefficients falls between. The agreement among the three analyses is consistent with the uncertainties in field heat budget monitoring, and in apartment temperature and wall U-value measurements. Possible sources of bias in the direct U-value measurement, mentioned previously, include sheltering by drapes, furniture, or dust, of wall surfaces peripheral to the HFMs[6]. Possible sources of bias in the UA obtained from the analysis of long-term monitored data include simplification of sol-air and window solar gains, simplification of thermal storage effects, simplification of the infiltration heating load submodel, apartment temperature sampling error, occupant load variations, window opening, and temperature, wind and enthalpy stream measurement errors.

CONCLUSION

Measured panel U-values are consistent with whole-building performance of two Ryazan demonstration buildings measured during the 1996-97 heating season. The measured U-values of walls in Petrozavodsk and Orenburg are typically lower (better) than those measured in Ryazan. This may indicate use of medium- or lightweight aggregates to obtain better thermal performance in these colder cities. The U-values in Zhukovskij are also better than those measured in Ryazan. Zhukovskij is not much colder than Ryazan but, being a center for aerospace R&D, was better positioned in the Soviet era to build quality housing.

While the potential for energy savings by exterior insulation is the highest of all possible retrofits, it is expensive and thus marginally cost effective. Furthermore, little of the envelope retrofit potential can be realized without improving control of heat delivery. Control at the building level is viable if the building distribution is properly balanced.

---

[6] Note that, consistent with the sheltering hypothesis, measured U-values of gable end walls, which generally have no drapes, are lower than the measured U-values for non-gable walls in the Petrozavodsk panel buildings. A genuine systematic U-value difference may also exist. The relative importance of these two effects cannot be determined without further field testing and, perhaps, modeling of the lateral heat flows.

Control at the heat substation level may be viable if all buildings served have close to the same solar/load ratio and balance point and distribution to buildings is properly balanced.

Engineering models used in the analysis of western buildings generally do not adequately handle important features of the EHDP buildings. Electricity represents the smallest, in terms of building heat balance, of EHDP utility energy streams. Other differences include large wall-section U-values, large distributed thermal mass, high and variable infiltration rates associated with leaky envelopes and uncontrolled natural ventilation. Building operational modes that are unfamiliar to western analysts include the large aperiodic indoor temperature variations and the significant fractions of the heat balance associated with cold water use, cooking gas use, and service hot water recirculation. Building thermal models must normalize for these operational differences as well as weather variations. EHDP impact evaluation must reflect changes in level of service.

A thermal response model based on the daily time series of building heat inputs, indoor temperature and daily average weather conditions was developed. The most important applicable thermodynamic constraint—zero sum of temperature coefficients—was imposed by a manipulation of the object function. It is impossible, without this constraint, to make meaningful inferences about the UA and thermal capacitance of the building represented by the model. We have derived a linear objective function that imposes the constraint by eliminating one of the temperature terms (one less degree of freedom). Thus the model can be applied by ordinary least squares methods. Application of the model to two nominally identical buildings with very different indoor temperature regimes indicates that it is very good at estimating the gross thermal parameters as well as being a good model for weather and indoor temperature normalization.

Key prerequisites to successful modeling are collection of complete and accurate data including temperatures of service hot water supply and return flows and of entering cold water and leaving waste-water flows. The need to measure these, as well as a sample of apartment temperatures, and to record daily use of gas, water and electricity at least doubles instrumentation costs with respect to basic revenue metering. Advances in metering and associated communications technologies will undoubtedly reduce the incremental cost in time. There is sufficient value in proper baselining and savings verification, nevertheless, to justify detailed monitoring of larger samples of EHDP buildings for at least one pre-retrofit heating season and for several post-retrofit seasons.

A similar constrained model was applied to the analysis of ASTM U-value test data. This application of the model is very rigorous. It does not eliminate the need for siting each HFM where heat flow is strictly one-dimensional (normal to both surfaces) all the way through the wall. It did, however, allow us to reliably characterize walls of high thermal capacitance per unit area with test periods of relatively short (3 days) duration.

ACKNOWLEDGMENTS

REFERENCES

Armstrong, P.R., J.A. Dirks, Y. Matrosov, J. Olkinaru, and D. Saum. 1996. "Infiltration and Ventilation in Russian Multi-Family Buildings." PNL-SA-28333, *ACEEE 1996 Summer Study on Energy Efficiency in Buildings*, August.

Armstrong, P.R., C.E. Hancock, and J.E. Seem. 1991. *Commercial Building Temperature Recovery—Theory, Experiment, and Design Procedure*, RP-491, *ASHRAE Trans.* 98(1).

ASHRAE 1993. *Handbook of Fundamentals*, Atlanta, GA.

ASTM C 518-76. *Standard test method for steady-state thermal transmission properties by means of a heat flow meter.* American Soc. for Testing and Materials, Philadelphia, PA.

ASTM C 1046-89. *Practice for calculating thermal transmission properties from periodic heat flux measurements.* American Soc. for Testing and Materials, Philadelphia, PA.

Birch and Krogboe. 1995. *Energy Saving Retrofits in Residential Buildings (Ryazan, Russia): Building Audit and Retrofit Analysis (Part A)*. B&K Project# EHDP/95-1/Russia, December.

BNW. 1996. Reilly, R.W., P.R. Armstrong, and L.A. Klevgard, Pre-Retrofit Energy Consumption--Ryazan Demonstration, Enterprise Housing Divestiture Project Report, May.

BNW. 1997a. Reilly, R.W., P.R. Armstrong, and L.A. Klevgard, Post-Retrofit Energy Consumption—Ryazan Demonstration, Enterprise Housing Divestiture Project Report, Jul.

BNW. 1997b. Armstrong, P.R., B.Y. Nekrasov, I. Sultanguzin, Infiltration Leak Characterization by Blower Door Tests, Letter Report to the FER, November.

BNW. 1998a. Armstrong, P.R., D.L. Hadley, J.A. Dirks, R.G. Lucas, R.W. Reilly, D.W. Winiarski. Infiltration and Ventilation Model for EHDP Buildings, report to the FER, January.

BNW. 1998b. Armstrong, P.R., J.A. Dirks, R.G. Lucas, B.Y. Nekrasov, D.W. Winiarski, V. Xhronchinkov. Measurement of Thermal Resistance of Apartment Building Walls in Four Russian Cities, report to the FER, May.

Dirks, J.A., R.W. Reilly, J.W. Currie, R. Dahowski, and P.R. Armstrong. 1996. "Building Energy Analysis and Retrofit Selection for Russian Multi-Family Housing," PNL-SA-28347, *ACEEE 1996 Summer Study on Energy Efficiency in Buildings*, August.

Drozdov, V.A., Yu.A. Matrosov, Yu.A. Tabunschikov. 1989. "Trends in energy efficiency of buildings--theory and practice in the USSR," Energy and Buildings, 14, 43-50.

EPRI. 1979. *Monitoring the Performance of Solar Heated and Cooled Buildings*, Volume 2, ER-1239, Electric Power Research Institute, November.

Fang, J.B. and R.A. Grot. 1985. "In-situ measurement of the thermal resistance of building envelopes in office buildings," *ASHRAE Trans* 91(1), paper CH-85-11-3.

Flanders, S.N. 1980. *Time Constraints on Measuring Building R-Values*, CRREL Report 80-15, US Army Corps of Engineers, Cold Regions Research and Engineering Laboratory.

Martinot, Eric 1997. *Investments to Improve the Energy Efficiency of Existing Residential FSU Buildings*, Worldbank Studies of Economies in Transformation 24, Washington, DC.

Matrosov, Yu.A., I.N. Butovsky and R.W. Watson. 1994. "Case Studies of Energy Consumption in Residential Buildings in Russia's Middle Belt Area." *Energy Build.*, 20(1).

Opitz, M.W., L.K. Norford, Yu.A. Matrosov, I.N. Butovskij. 1997. "Energy consumption and conservation in Russian apartment building stock," Energy and Buildings, 25, 75-92.

Stephenson, D.G. and G.P. Mitalas. 1971. "Calculation of heat conduction transfer functions for multi-layer slabs," *ASHRAE Trans* 77(2).

Whittle, D., M. Kuraishi, and L. Freinkman. 1996. *Staff Appraisal Report: Russian Federation Enterprise Housing Divestiture Project*, Worldbank int. doc. 15112-RU, April.

Zhuze, V.B. 1996. *Preliminary ECOs--Estimation of Some Recommended Technologies*, Field inspection report, 22 Oct. 1996, FER report, Center for Energy Efficiency, Moscow.

APPENDIX A: TIME SERIES MODEL OF TRANSIENT THERMAL CONDUCTION

A number of errors can affect U-value test results. Some, such as poor or variable thermal contact between wall surface and sensor, or inconsistent response to convection and radiative heat exchange, are associated with installation. Others, such as small average temperature difference, a persistent trend spanning the test period, or inadequate test duration, are associated with test conditions. A third category, which includes such questions as selection of time-step size, model form and model order, is the *method of analysis* or *modeling* approach. This appendix describes a model formulation that addresses the problem of marginal test conditions. We will not address the more general questions of sampling error and experimental design (sample size and selection), which are adequately covered in statistics texts, or the problems of lateral heat transfer and selection of appropriate test points, which are also treated elsewhere (ASTM; EPRI 1979; Fang and Grot 1985; Flanders 1980).

The simplest U-value estimate is a ratio of heat flux to temperature difference:

$$U = \frac{\overline{q}}{\overline{T_x} - \overline{T_z}} = \frac{\sum q}{\sum T_x - \sum T_z}$$

where

q = surface heat flux (Wm^{-2}),

T_x = exterior surface temperature (C), and

T_z = interior (zone-side) surface temperature (C).

This estimate does not account for a change in stored energy. The U-value error caused by this storage effect is the change in stored energy per unit wall area expressed as a fraction of the net energy per unit area conducted through the wall over the duration of the test. Five factors affect the magnitude of this error: thermal capacitance and U-value of the wall, duration of the test, average temperature difference during the test, and temperature change between start and end of the test. For walls with a 12-hour or longer time constant, the error can exceed 20% in a 3-day test.

Measurement of a wall's internal energy is difficult even in a laboratory environment because the temperature profile of each of the wall's components must be measured and the thermal capacitance of each component must be known. Internal energy measurement in the walls of occupied apartments is generally not feasible. Two practical ways to reduce thermal storage errors are to: 1) arrange for long duration tests with large average temperature difference across the wall and small temperature change from start to end of test, or 2) use time series analysis to internalize the storage effects. The latter approach, once properly implemented in software, has the obvious advantage of increasing the number of tests that can be performed in a given time period with a given set of expensive test equipment.

The conduction transfer function (CTF) model (Stephenson and Mitalas 1971), used by nearly all thermal simulation programs, is a practical, rigorous time-series model of the conduction process. The CTF is attractive for analysis of time-series U-value data because of its linear form:

$$q_o = \sum_{i=1}^{n} C_{q,i} q_i + \sum_{i=0}^{n} C_{x,i} T_{x,i} - \sum_{i=0}^{n} C_{z,i} T_{z,i}$$

where the index subscripts attached to heat flux, q; exterior surface temperature, T_x; and interior surface temperature, T_z, refer to their (lagged) values i time steps previous. Similarly, C_q, C_x, and C_z are CTF coefficient vectors whose elements are associated with past temperatures and heat fluxes by the same i index. Note that a large number of CTF models, with different time step size and model order, can be fit to a given time series of wall thermal response data. Our goal is to select the sub-set of fitted models that best represent a wall's thermal response. Lower order models that do not represent all the significant time constants may give a U-value estimate that is biased by thermal storage effects. Models of too high an order tend to represent features of the driving functions or noise in the data—a condition sometimes called *overfitting*. The implied thermal capacitance often changes abruptly when the model order reaches the point where such overfitting first occurs.

Derivation of the CTF model from first principles leads to q, T_x, and T_z terms each involving the same number (n) of past values. This inverse modeling restriction alone, however, is not enough to preclude a fitted model that, while providing a reasonable qualitative match to the measured response, still violates Fourier's law of conduction. Consider the CTF subjected to steady indoor and outdoor temperatures. Now q_i, $T_{x,i}$, and $T_{z,i}$, being invariant with i, can be taken outside their summations:

$$q(1 - \sum_{i=1}^{n} C_{q,i}) = T_x \sum_{i=0}^{n} C_{x,i} - T_z \sum_{i=0}^{n} C_{z,i} \text{ or, equivalently}: q = \frac{T_x \sum_{i=0}^{n} C_{x,i} - T_z \sum_{i=0}^{n} C_{z,i}}{1 - \sum_{i=1}^{n} C_{q,i}}$$

For the model's steady-state response to fit the definition of a U-value, $U = q/(T_x - T_z)$, the temperature coefficients must be equal. Thus, if

$$\sum_{i=0}^{n} C_{x,i} = \sum_{i=0}^{n} C_{z,i} \text{ we can write}$$

$$q = \frac{(T_x - T_z) \sum_{i=0}^{n} C_{x,i}}{1 - \sum_{i=1}^{n} C_{q,i}} \text{ which can be arranged in the desired form}: U = \frac{q}{T_x - T_z} = \frac{\sum_{i=0}^{n} C_{x,i}}{1 - \sum_{i=1}^{n} C_{q,i}}$$

It turns out that this constraint can be imposed on the CTF temperature coefficients by using a transformed data set in which one of the lagged temperatures is subtracted from all others. To accomplish this, isolate one of the temperature, say $T_{z,0}$; the model then becomes:

$$q_0 = \sum_{i=1}^{n} C_{q,i} q_i + \sum_{i=0}^{n} C_{x,i} T_{x,i} - \tilde{N}_{z,0} T_{z,0} - \sum_{i=1}^{n} C_{z,i} T_{z,i}$$

Now make the subsitution $C_{z,0} = \sum_{i=0}^{n} C_{x,i} - \sum_{i=1}^{n} C_{z,i}$ to obtain the constrained linear model :

$$q_0 = \sum_{i=1}^{n} C_{q,i} q_i + \sum_{i=0}^{n} C_{x,i} (T_{x,i} - T_{z,0}) - \sum_{i=1}^{n} C_{z,i} (T_{z,i} - T_{z,0}).$$

APPENDIX B: TIME SERIES MODEL OF WHOLE-BUILDING HEAT BALANCE

The desired steady-state form of the building heat balance model is:

$$Q + k_S * S = k_W * W * dT + k_T * dT$$

where

Q is the net energy provided by gas, electric, heat and water utilities (W),

k_S, k_W, k_T are aggregate regression coefficients,

S is the daily average solar radiation (Wm^{-2}) incident on the horizontal,

W is the average daily wind speed (m/s),

dT is the average indoor-outdoor temperature difference (K).

If we consider the wind-driven infiltration to be part of the instantaneous heat load, we can write the transient heat balance equation in terms of thermal response factors as:

$$Q + k_S * S + k_W * W * (-dT) = SUM(k_{z,i} T_{z,i} - k_{x,i} T_{x,i})$$

where the right-hand side is the sum of an infinite converging series involving past indoor and outdoor temperatures. It is convenient to follow the common sign convention in which all heat flows into the building are positive and to collect left-hand heat load terms thus:

$$Q_0 = \sum_{i=0}^{\infty} C_{x,i} T_{x,i} - \sum_{i=0}^{\infty} C_{z,i} T_{z,i}$$

where the subscript 0 denotes current time and i denotes number of time steps into the past. The response factor form is, for a linear lumped-parameter system, equivalent to the transfer function form:

$$Q_0 = \sum_{i=1}^{n} C_{Q,i} Q_i + \sum_{i=0}^{n} C_{x,i} T_{x,i} - \sum_{i=0}^{n} C_{z,i} T_{z,i}$$

which is identical to the CTF form presented in Appendix A. One may legitimately expect the model order for whole-building thermal response to be much higher than that for thermal response of a single wall. After all, a building subsumes a different set of time constants for each wall type used in its construction, the time constants associated with all kinds of contents, as well as the time constants of internal walls, decks, and other structures. However, it has been shown (see literature review in Armstrong et al. 1991) that reduced order models will reproduce the behaviors of high order thermal systems quite well in most cases. The transformation (derived in Appendix A) that allows one to obtain the CTF model coefficients by linear regression while imposing the zero sum constraint on temperature coefficients can be applied directly to the whole-building transfer function.